

Method for noise-induced regularization in quantum neural networks

Wilfrid Somogyi, Ekaterina Pankovets, Viacheslav Kuzmin, and Alexey Melnikov
Terra Quantum AG, 9000 St. Gallen, Switzerland

(Dated: October 29, 2024)

In the current quantum computing paradigm, significant focus is placed on the reduction or mitigation of quantum decoherence. When designing new quantum processing units, the general objective is to reduce the amount of noise qubits are subject to, and in algorithm design, a large effort is underway to provide scalable error correction or mitigation techniques. Yet some previous work has indicated that certain classes of quantum algorithms, such as quantum machine learning, may, in fact, be intrinsically robust to or even benefit from the presence of a small amount of noise. Here, we demonstrate that noise levels in quantum hardware can be effectively tuned to enhance the ability of quantum neural networks to generalize data, acting akin to regularisation in classical neural networks. As an example, we consider a medical regression task, where, by tuning the noise level in the circuit, we improved the mean squared error loss by 8%.

I. INTRODUCTION

Recently, significant progress has been made in developing quantum processing units (QPUs) [1–3]. However, the current generation of QPUs is still characterized by relatively short coherence times. Executing algorithms on these so-called noisy intermediate-scale quantum (NISQ) devices [4, 5] often requires significant error mitigation to combat the effects of decoherence and noise-induced errors [6–8].

Variational quantum algorithms (VQAs) are designed to operate within the constraints of NISQ devices. However, VQAs cannot completely ignore the noise that arises on QPUs. The headway has been made in understanding the effects of specific types of noise, including those described by phase-damping, depolarizing, and amplitude-damping channels, as well as leakage error, shot noise, and coherent Gaussian noise [9–12]. While noise typically poses challenges to VQAs, it can also be advantageous for specific quantum algorithms. For instance, it has been shown that stochastic noise aids in avoiding saddle points [13] in variational circuit optimization, quantum noise protects quantum classifiers against adversarial attacks [14], and noise reduces the number of gates in reservoir computing [15]. In this work, we further investigate the potential benefits of quantum noise by developing a practical method for regularizing quantum machine learning models using the noise naturally present in quantum hardware.

In classical machine learning, exploiting noise is known to be a tool to prevent so-called overfitting. The issue of overfitting is a well-recognized challenge, occurring when a model achieves strong performance on the training dataset but struggles to generalize the unseen data. Overfitting occurs when a model captures noise or irrelevant patterns in the training data rather than the underlying true patterns that generalize across datasets. To mitigate this issue, the strategies of adding noise into the data, weights, or gradients have been proposed [16–18].

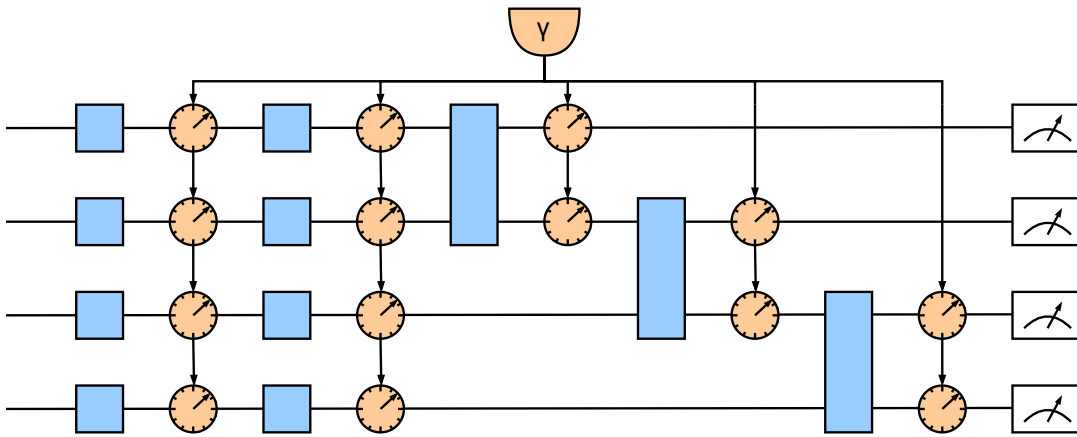


FIG. 1: Scheme of the method for regularising QNN models proposed in the work. Blue rectangles indicate single and two-qubit gates. Orange circles after each gate indicate the action of induced controllable noise with the strength optimized as a regularisation hyperparameter.

The observed effectiveness of noise in preventing overfitting in classical machine learning suggests its potential utility in mitigating overfitting in quantum neural networks [19, 20] (QNNs). Recently, it has been demonstrated that adding noise to initial data or to the weights of QNN can act as a regularisation similar to its classical counterpart. For instance, in [21], the approach of adding noise to the quantum kernel method was explored. The proposed method operates as follows: initial data undergoes processing through a quantum circuit, after which the density matrix is measured, and the outputs are subsequently fed into a linear model. It appeared that adding noise at the quantum circuit stage helps to reduce overfitting. Notably, within this method, noise is incorporated during the data encoding process before training, which corresponds to the introduction of noise into the initial data. The idea of using noise as a tool to mitigate overfitting in QNNs was also investigated in [22]. The QNN model employed in this paper involves tuning the parameters of the Hamiltonians to guide the evolution toward a state that yields a target expectation value. In this paper, noise is added to the initial data, and the noise model is implemented as a Gaussian perturbation of the elements of the initial density matrix. Furthermore, the authors investigated the scenario of introducing noise into the weights of the model. In both instances, their model exhibited improved generalization performance in the presence of noise.

In this paper, we complement the existing techniques by proposing an approach to leverage quantum noises, which naturally occur in quantum devices, to prevent overfitting. We suggest a method, schematically shown in Fig. 1, of adding one or several of the noise channels accessible in available quantum hardware. Adjusting the noise rates as hyper-parameters allows one to obtain a model that is superior to the noiseless scenario. We numerically investigate this method for a regression task by using several modeled noise channels and demonstrate improvement in the generalization performance. Finally, we discuss the practical implementation of the method in real quantum hardware.

II. DECOHERENCE

In this section, the mathematical definitions are given for three quantum noise channels studied in the paper. Namely, the amplitude-damping, phase-damping, and depolarizing channels. The relationship between these fundamental channels and the statistics commonly quoted to characterize quantum hardware are also described.

Decoherence arises as a result of the interaction between a quantum system and its environment. In the case of quantum processing units, the quantum state of the environment is not well known, and as a result, the state of the system qubits must be described in terms of the density matrix formalism. In general, the state of an N qubit system interacting with its environment can be described by the density matrix ρ

$$\rho = \sum_j p_j |\psi_j\rangle\langle\psi_j| \quad (1)$$

which denotes a probabilistic ensemble of pure states $|\psi_j\rangle$ where p_j is the probability that the state of the system is $|\psi_j\rangle$. An evolution on this system can, in turn, be described in terms of a set of Kraus operators, E_k , which act on the density matrix as follows

$$\mathcal{E}(\rho) = \sum_k E_k \rho E_k^\dagger \quad (2)$$

where the set of operators $\{E_k\}$ describe the quantum operation \mathcal{E} , often referred to as a ‘quantum channel’, and obey the completeness relation $\sum_k E_k^\dagger E_k = \mathbb{I}$.

Amplitude-damping corresponds to *energy loss* to the environment and describes the probability of the system in the state $|1\rangle$ decaying into the state $|0\rangle$. This channel is described by the following set of Kraus operators:

$$E_0 = \begin{bmatrix} 1 & 0 \\ 0 & \sqrt{1 - \gamma_{AD}} \end{bmatrix} \quad (3)$$

$$E_1 = \begin{bmatrix} 0 & \sqrt{\gamma_{AD}} \\ 0 & 0 \end{bmatrix} \quad (4)$$

Phase-damping represents a type of noise that destroys quantum coherence, and corresponds to a contraction of the Bloch sphere in the $x-y$ plane. This results in a destruction of quantum superpositions in the limit $\gamma_{PD} \rightarrow 1$, and a density matrix that describes entirely classical probability distributions of the states $|0\rangle$ and $|1\rangle$. The phase-damping channel is described by the following set of Kraus operators:

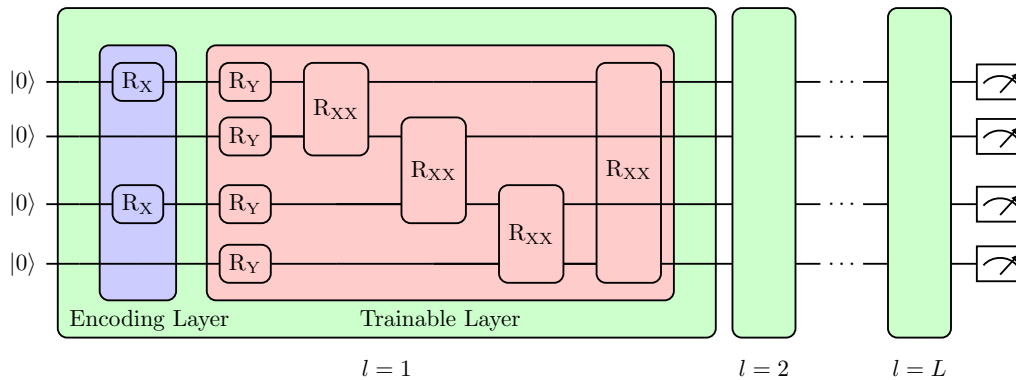


FIG. 2: The ansatz used to construct the QNN model, with alternating encoding and trainable layers, followed by a simultaneous Pauli-Z measurement on all four qubits. Features are encoded with RX gates on the odd-numbered qubits. The trainable layers is composed of a series of single-qubit RY gates followed by a ring of two-qubit RXX gates. Here we depict a model with depth L .

$$E_0 = \begin{bmatrix} 1 & 0 \\ 0 & \sqrt{1 - \gamma_{PD}} \end{bmatrix} \quad (5)$$

$$E_1 = \begin{bmatrix} 0 & 0 \\ 0 & \sqrt{\gamma_{PD}} \end{bmatrix} \quad (6)$$

Depolarizing corresponds to the qubit experiencing an ‘error’ with probability γ_{DP} . The possible types of error are the phase flip (E_1), bit flip (E_2), or phase-bit flip (E_3). In this case, the Kraus operators are the identity matrix and the three Pauli matrices:

$$E_0 = \sqrt{1 - \gamma_{DP}} \begin{bmatrix} 1 & 0 \\ 0 & 1 \end{bmatrix} \quad (7)$$

$$E_1 = \sqrt{\frac{\gamma_{DP}}{3}} \begin{bmatrix} 1 & 0 \\ 0 & -1 \end{bmatrix} \quad (8)$$

$$E_2 = \sqrt{\frac{\gamma_{DP}}{3}} \begin{bmatrix} 0 & 1 \\ 1 & 0 \end{bmatrix} \quad (9)$$

$$E_3 = \sqrt{\frac{\gamma_{DP}}{3}} \begin{bmatrix} 0 & -i \\ i & 0 \end{bmatrix} \quad (10)$$

III. TRAINING

The effect of decoherence on QNNs is explored via the diabetes dataset, which is commonly employed in the field of classical machine learning and readily accessed through various common software libraries, including `scikit-learn` Python package [23]. The *diabetes* dataset consists of information from a study of 442 diabetes patients [24]. The dataset contains 10 baseline variables and the response of interest, which is a quantitative measure of disease progression one year after the baseline measurements. The target feature is the response of interest, and the baseline variables constitute the predictive data features: age in years, body mass index, average blood pressure, total serum cholesterol, low-density lipoproteins, high-density lipoproteins, total cholesterol, log of serum triglycerides level, and blood sugar level. From these ten features, the bmi and log of serum triglycerides level (ltg) are selected as the two features on which the models are trained. A random subset of the data is partitioned into 40 training samples and 400 validation samples. The predictive features are scaled in the range $[-\pi, \pi]$, and the target feature is scaled in the range $[-1, 1]$ using the `scikit-learn` `MinMaxScaler`. The scaling coefficients are obtained based on the training dataset, and the validation dataset is scaled accordingly to avoid any information leakage from the validation dataset to the training dataset.

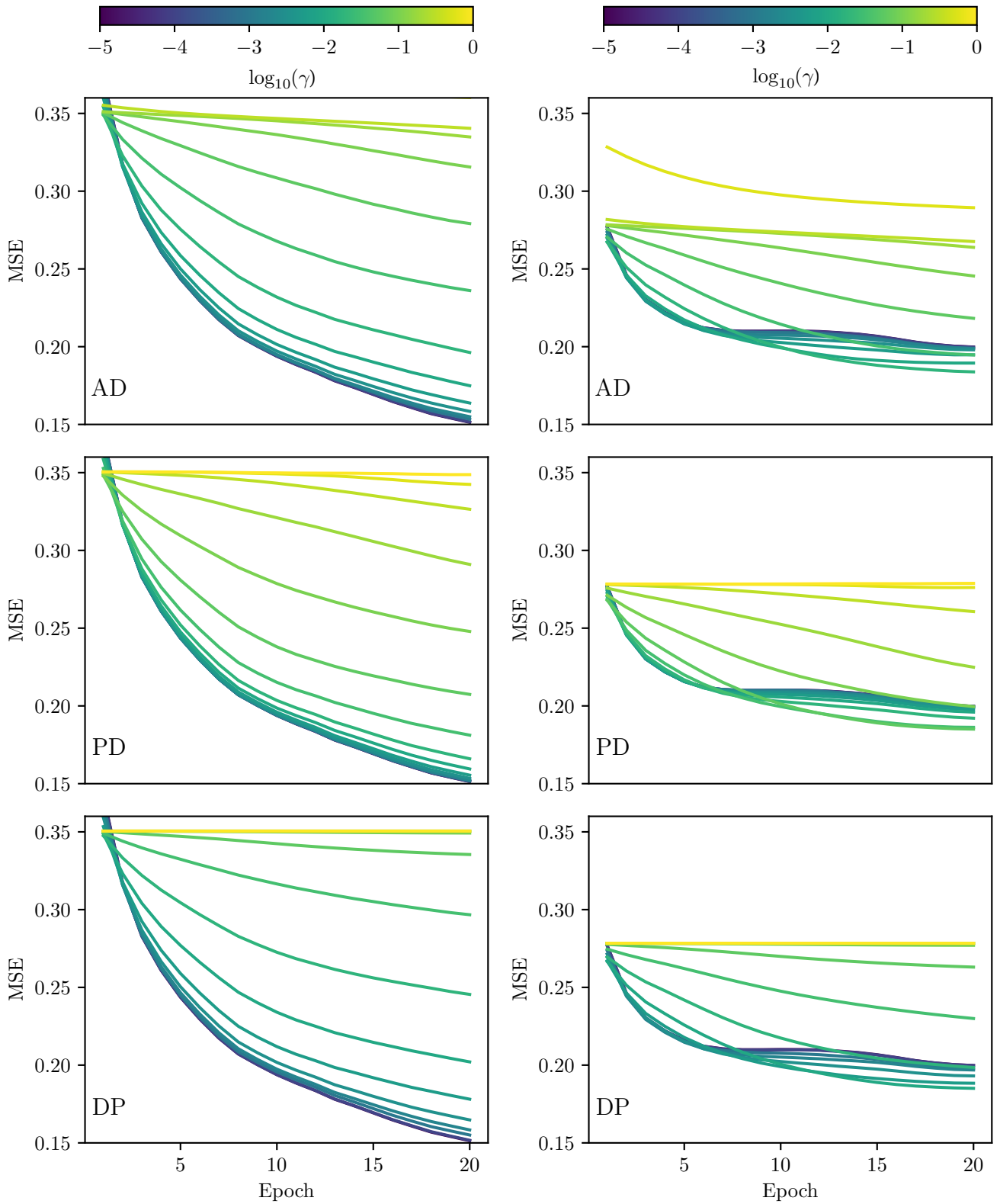


FIG. 3: The average MSE of the training (left) and validation (right) datasets across all 20 training epochs shown for each value of the noise parameter γ for each noise channel. From top to bottom the noise channels shown are the amplitude damping (AD), phase damping (PD) and depolarizing (DP) channels. The lines are coloured according to the logarithmic value of γ .

Various QNN ansätze can be designed in search of a solution to some quantum machine learning task. In general, all QNNs are formed by a series of parameterized quantum gates acting on some register of quantum and optionally classical bits. However, they can be broadly categorized into three ‘species’: dissipative QNNs [25], in which information is transferred to a new register of qubits at each layer (analogous to a classical feed-forward neural network); convolutional QNNs [26, 27], where some number of qubits are measured at each layer to reduce the dimension of the data; and ‘standard’ QNNs [28–32], in which the number of qubits remains constant throughout. Of the three, the latter type of QNN is the most commonly used throughout the literature for quantum machine learning tasks. For that reason a similar architecture is chosen for the present study. Our ansatz, shown in Fig. 2, consists of four qubits, initially prepared in the $|0\rangle$ state. Two data features are then encoded on the first and third qubits, respectively, via two RX gates, referred to as the feature encoding layer. The feature encoding layer is followed by a layer of single qubit RY gates and a ring of symmetric RXX Ising gates, referred to as the trainable layer. The alternating feature encoding and trainable layers can be repeated L times for a total depth of $4L$ gates per qubit. Finally, a simultaneous Pauli-Z measurement is performed on all four qubits, and the expectation value $\langle Z^{\otimes 4} \rangle$ is interpreted as the normalized prediction value. The quantum circuit is created using the PennyLane Python package and subsequently wrapped as a Torch layer using `pennylane.qnn.TorchLayer` [33].

To assess the impact of quantum decoherence on the training process of a QNN, the strength of the three quantum noise sources described in Sec. II is varied independently for 15 values of p according to the following distribution

$$\gamma = 10^p \quad p \in [-5, 0]. \quad (11)$$

For each value of γ , 16 randomly initialized models are trained on a random subset of the entire dataset consisting of 40 training samples. A further 400 samples from the dataset are selected to form the validation dataset.

The quantum model is trained using batch gradient descent, with a batch size of 20 and the training dataset is randomly permuted at each training epoch in order to randomize the samples in each batch across epochs. The trainable parameters of the model are optimized by gradient descent using an Adam optimizer to minimize the mean squared error (MSE) loss. The Adam optimizer is initialized with a learning rate $\gamma = 0.03$, beta coefficients $\beta_1 = 0.9$ and $\beta_2 = 0.999$, and a weight decay parameter $\lambda = 0$. Both the loss function and optimizer are standard components of the PyTorch library [34, 35]. At each epoch, the prediction accuracy of the model is also measured by executing the model in the feed-forward mode and calculating the average MSE across all 400 samples in the validation dataset.

IV. RESULTS

The results of the training process of the model with $L = 5$ layers and 40 variational parameters, described in Sec. III, are shown in Fig. 3, which depicts the mean test and training set losses across all 16 models at each epoch for varying strengths of the three noise channels.

Initially, we note that very high levels of noise reduce the ability of the model to accurately characterize a dataset, which is evidenced by the reduction in the gradient of the loss curves for values of $\gamma > 0.1$. This is a consequence of the fact that the measurement outcome of the quantum circuit becomes increasingly uncorrelated with the input data features as noise in the quantum circuit increases. Consider the case of the amplitude-damping channel, described by Eqs. (3) and (4). It is straightforward to see that in the limit of $\gamma \rightarrow 1$, the state $|0\rangle$ will be measured with unit probability. Thus, the model predicts the value $\hat{y} = 1$ for all values of the input features. Moreover, calculating the average MSE error loss across all samples in the dataset for a model which always predicts the value $y = 1$, one obtains

$$\sum_i^M \frac{\mathcal{L}(y_i, 1)}{M} = 1.706 \quad (12)$$

which is indeed the value of the loss function in the case $\gamma_{AD} = 1.0$ (see Fig. 4). Similarly, a naive model that predicts the value $\hat{y} = 0$ for all values of the input features gives an average MSE loss of $\mathcal{L} = 0.278$, which is the value obtained in the limit $\gamma_{PD} \rightarrow 1$ or $\gamma_{DP} \rightarrow 1$.

These results are not particularly surprising. What is more interesting is the behavior observed when the level of noise is small but non-zero. In Fig. 4, the loss curves for the training dataset can be seen to increase monotonically with respect to the level of noise. However, the MSE loss curve for the validation dataset exhibits a minimum for some finite value of γ greater than zero. Intuitively, one might expect that any level of noise results in a degradation in the performance of a QNN. However, the results presented here imply that the relationship between quantum decoherence

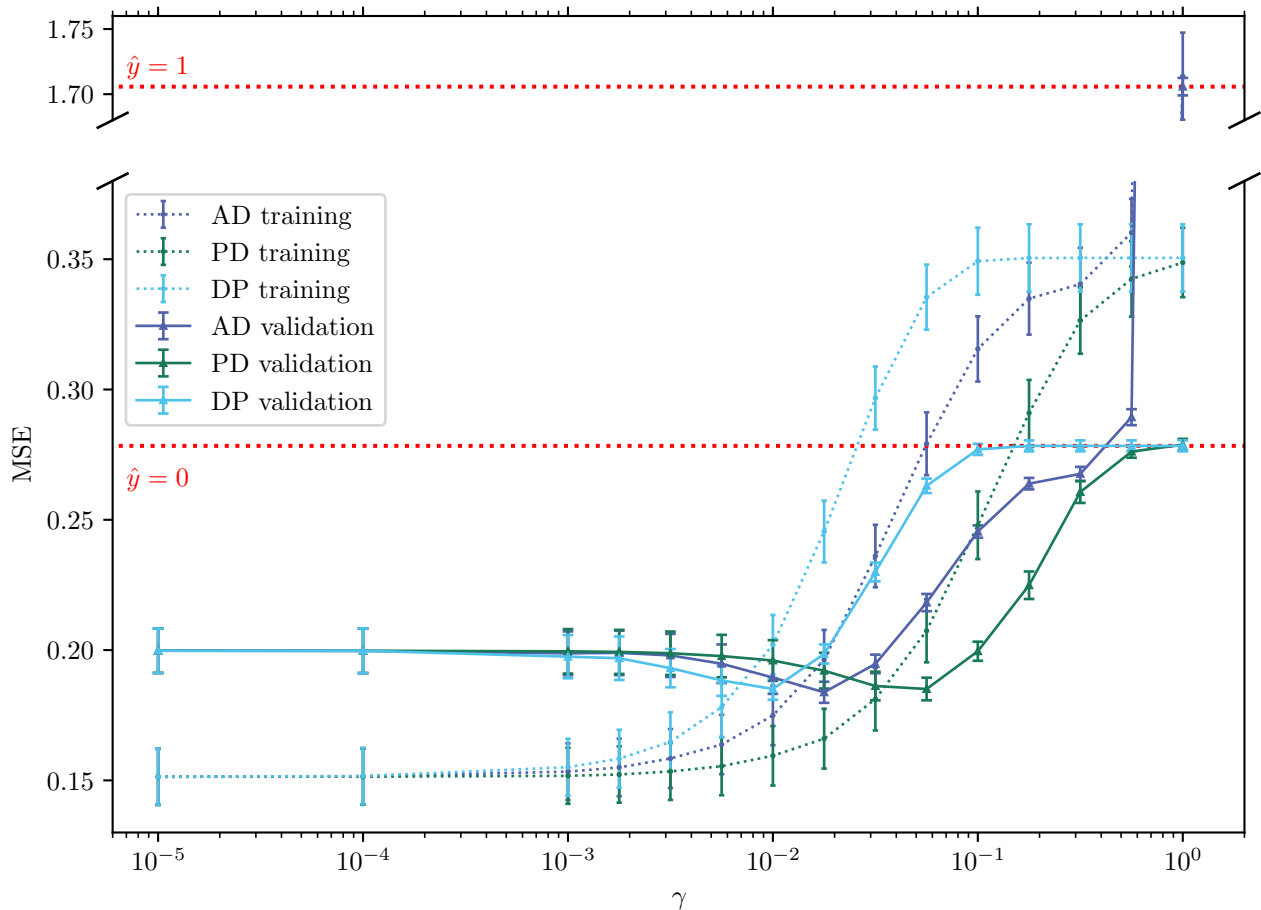


FIG. 4: The mean final MSE loss after training 16 instances of the QNN model described in Sec. III, with $L = 5$ layers, on the diabetes dataset, as a function of the noise parameter γ for each of the three noise channels. The solid lines represent the MSE of the validation dataset, while the dotted lines represent the MSE of the training dataset. Vertical error bars show the standard error across all 16 models. Two horizontal lines are also plotted, indicating the loss of naive models that predict $\hat{y} = 0$ and $\hat{y} = 1$ for all inputs.

and the ability of a QNN model to accurately predict features of a dataset is not straightforward. Moreover, we show that a model trained in the presence of some small amount of quantum noise can exhibit improved performance relative to a model trained in a noiseless environment. In the case of the model problem outlined in Sec. III, we observe a maximum 8.0% improvement in the model's ability to characterize the validation dataset relative to the noiseless model when the level of amplitude damping noise is $\gamma = 10^{-1.75}$. In the case of the phase damping and depolarizing channels, the optimum level of noise occurs for $\gamma = 10^{-1.25}$ and $\gamma = 10^{-2.00}$, respectively, each with a 7.4% reduction in the loss.

Finally, we note that the noiseless models in Fig. 3 exhibit a pattern reminiscent of the double descent phenomenon [36] in the validation loss. While the noise level increases, this pattern gradually disappears, displaying behavior similar to one observed in regularised classical neural networks, as shown in Fig. 22 of Ref. [36].

A. Feed-Forward Noise Map

Understanding the impact of varying noise levels on the model's performance in feed-forward mode is crucial. To investigate this, we initially train 16 models in the presence of noise γ_T for each noise channel. Subsequently, we fix the models' weights and evaluate their performance on the validation dataset in feed-forward mode, where the noise level γ_F may differ from γ_T . Specifically, we vary the values of γ_T and γ_F according to the distribution mentioned earlier (Eq. (11)), yielding a two-dimensional mapping that provides insights into the optimal noise level (γ_F) for

feed-forward mode, given a model trained in the presence of a given level of noise (γ_T).

In Fig. 5, we show the 2-dimensional map of the MSE loss for each of the three noise channels. In addition to this map, Fig. 6 shows the value of γ_T , which provides the minimum MSE loss for each value of γ_F . The most notable feature is seen for models executed in the feed-forward model with the depolarizing channel when $\gamma_F = \mathcal{O}(0.01)$. For these models, the lowest MSE loss is observed when γ_T is marginally larger than γ_F . This suggests that, in some cases, the optimum performance for a QNN model executed on a noisy quantum computer can be achieved by increasing the level of noise during the training process.

V. QUANTUM NOISE REGULARIZATION

In the context of the results outlined in Fig. 4, we propose that noise can be considered as a type of ‘quantum regularization.’ The observation that the presence of a small amount of noise enhances the performance of the validation dataset while showing no improvement on the training dataset (as depicted in Fig. 4) indicates that noise can have an effect analogous to the techniques of regularization commonly employed in classical machine learning. In other words, the noise described in Sec. II has the ability to reduce the degree of overfitting and improve the model’s ability to predict unseen data. In order to leverage this effect, we propose a method that allows for the level of noise in a QNN to be treated as a hyperparameter of the optimizer applied in the training phase by augmenting the quantum circuit with additional quantum gates or by the introduction of artificial noise. This method is applicable to both quantum emulators and quantum processing units:

1. An initial hybrid or fully quantum ansatz is specified based on some problem-specific criteria.
2. Sources of quantum noise describing one or more quantum decoherence channels are then inserted into the ansatz after each gate operation.
3. An input parameter is provided to these sources, enabling the adjustment of the level of decoherence γ .
4. The value of the input parameter is then chosen based on performance metrics of the QNN applied to the problem, e.g
 - Through the use of some optimization routine that minimizes the validation loss or some equivalent metric.
 - Through a systematic selection of the noise parameter based on holistic constraints.

In essence, the method seeks to adapt a variational quantum algorithm in such a way that the degree of noise in the circuit becomes a hyper-parameter of the ansatz.

A. Introducing Additional Noise

In the procedure outlined above, the method by which noise is introduced to a quantum circuit was defined abstractly. In this section we seek to outline some concrete ways in which this can be achieved.

In the case of quantum emulators, a specific level of noise can be achieved straightforwardly within the density matrix representation using the Kraus operator formalism for a given quantum channel. Some examples of these quantum channels were given in Sec. II. In this case, the boxes depicted in Fig. 1 take the form of parameterized Kraus operators.

On the other hand, controlling the amount of noise above some minimum (set by the intrinsic level of hardware noise) for a physical QPU is not straightforward. When comparing the optimum levels of noise across different circuit depths to the measured coherence times for popular quantum processing units (Table II), it is apparent that the level of noise present on many quantum devices is lower than the level of noise required to achieve optimum performance for some quantum machine learning problems. These values are shown, respectively, in Tables I and II for each of the three channels. Moreover, the optimum level of noise for producing the regularization phenomenon is observed to be approximately constant with the increasing number of ansatz layers.

Decoherence rates can be obtained experimentally and thus are commonly used by QPU vendors as a metric for noise robustness. Two decoherence rates are usually quoted, the so-called relaxation time T_1 and the dephasing time T_2 , which are closely related to two of the fundamental channels outlined in Sec. II. Given the single qubit gate execution time, T_G , and the value of T_1 or T_2 , one can estimate the value of the noise parameter γ for the *amplitude-damping* and *phase-damping* channels respectively. In practice this means the degree of amplitude damping and phase damping noise can be increased by artificially extending the gate execution time through the addition of idle time following each gate operation.

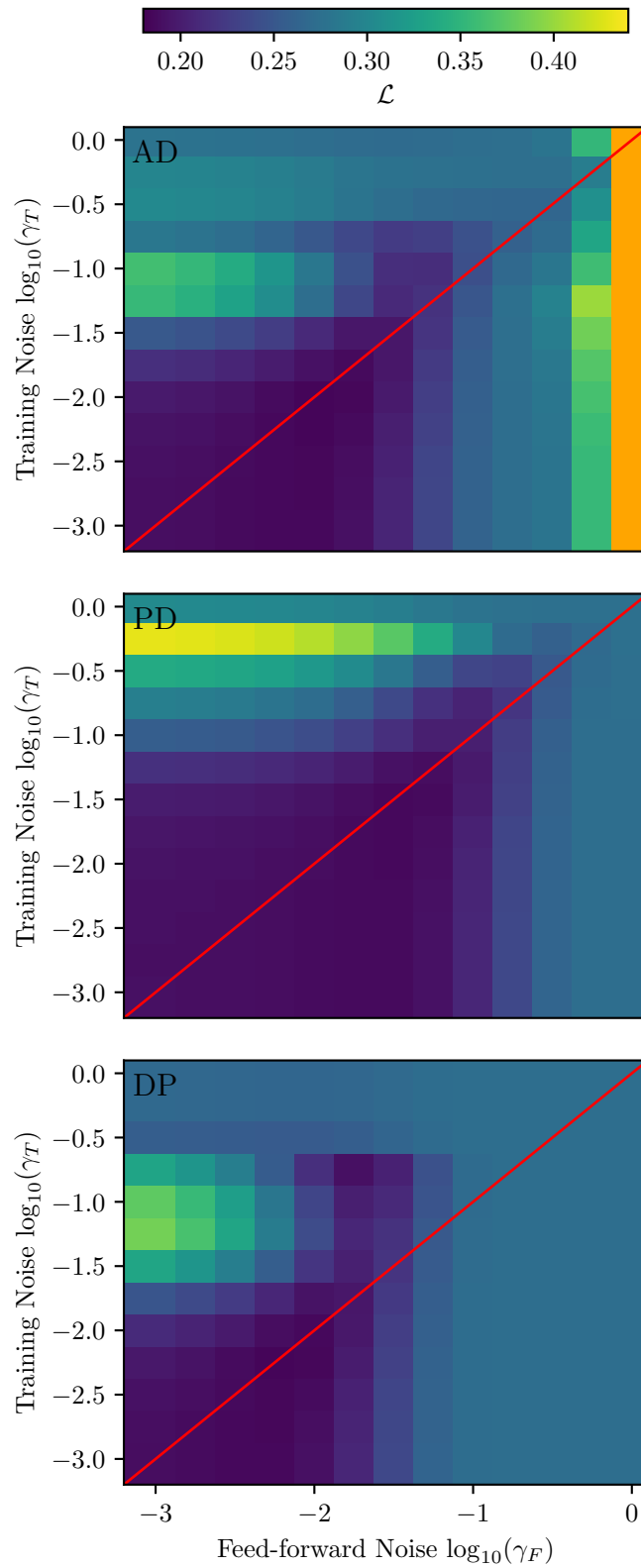


FIG. 5: The noise mapping shows the MSE loss for models where the level of noise differs between the training and validation environments. The orange color for $\gamma_F = 1$ indicates a value of 1.706. The diagonal red line illustrates the position of models that are validated with the same level of noise as they were trained.

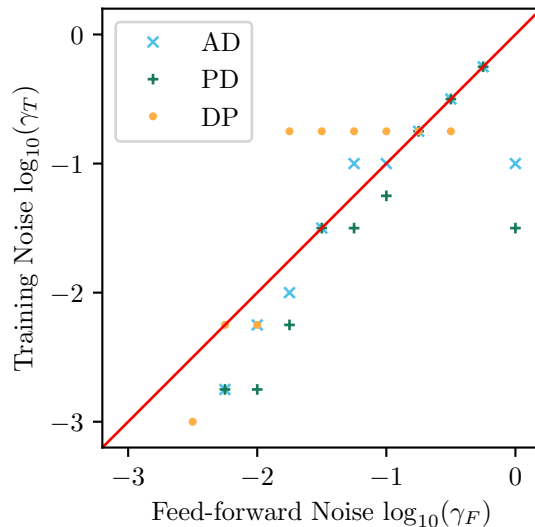


FIG. 6: The training noise level (γ_T) corresponds to the minimum MSE observed during testing on the validation dataset with noise level γ_F . In other words, this plot indicates the set of points (γ_F, γ_T) , s.t. the best performance during testing with noise γ_F is achieved when the model is preliminary trained with noise level γ_T .

Noise Channel	Mean Optimum Noise	$L = 3$	$L = 4$	$L = 5$	$L = 6$	$L = 8$	$L = 10$
γ_{AD}	1.00×10^{-2}	1.78×10^{-2}	1.78×10^{-2}	1.78×10^{-2}	1.00×10^{-2}	1.00×10^{-2}	1.31×10^{-2}
γ_{PD}	3.16×10^{-2}	3.16×10^{-2}	5.62×10^{-2}	3.16×10^{-2}	3.16×10^{-2}	1.78×10^{-2}	3.38×10^{-2}
γ_{DP}	5.62×10^{-3}	5.62×10^{-3}	1.00×10^{-2}	5.62×10^{-3}	5.62×10^{-3}	5.62×10^{-3}	6.50×10^{-3}

TABLE I: The average optimum noise parameter for the three noise channels across circuits of variable depth with $3 \leq L \leq 10$ layers.

In the case of the *depolarizing* channel, additional noise can be introduced by mimicking the effect of the depolarizing channel with single-qubit Pauli operators. The Kraus operators in Eqs. (7) - (10) correspond to the identity operator and the three Pauli operators (I, X, Y, Z). Thus, the effect of additional depolarizing noise can be achieved using a random number generator that applies one of the Pauli operators with probability $\gamma/3$ or the identity operator with probability $1 - \gamma$.

$$\gamma_{AD} = 1 - \exp\left(-\frac{T_G}{T_1}\right) \quad (13)$$

$$\gamma_{PD} = 1 - \exp\left(-\frac{T_G}{T_2}\right) \quad (14)$$

Hardware	T_1	T_2	T_G (2Q)	γ_{AD}	γ_{PD}
Rigetti Aspen M-3 [37]	25.0 μ s	28.0 μ s	240 ns	9.55×10^{-3}	8.54×10^{-3}
IonQ Aria [38, 39]	10 s	1 s	600 μ s	6.00×10^{-5}	6.00×10^{-4}
Google Sycamore [40]	15 μ s	19 μ s	12 ns	8.00×10^{-4}	6.31×10^{-4}
IBM Osprey Seattle [41]	85.9 μ s	63.0 μ s	635 ns	7.37×10^{-3}	1.00×10^{-2}

TABLE II: The average amplitude damping and phase damping noise for various QPUs, obtained via Eqs. (13) and (14) from coherence times provided by the vendors.

VI. CONCLUSION

This work presents a study of the effect of the three most common noise channels on QNNs. We explore how adjusting the levels of amplitude damping, phase damping, and depolarizing noise within a quantum circuit influences a QNN’s capacity to learn and generalize data. As an example, we considered a medical regression task, where, by tuning the noise level in the circuit, we improved the mean squared error loss by 8%. Our observation reveals that introducing a certain degree of decoherence throughout the circuit can effectively prevent overfitting. Building upon these findings, we propose a technique that leverages noise to enhance the generalization performance of QNNs.

The practical implementation of our technique presents challenges, particularly when transitioning from optimization on simulation to quantum hardware. While we have shown for a particular task that the optimal noise level required to prevent overfitting is lower than the noise level of the hardware, there may be instances where the opposite holds true. In such cases, introducing additional noise would degrade performance rather than enhance it. However, this issue might be solved by using a different quantum circuit architecture or by adjusting the level of error mitigation. These findings suggest that it would be valuable to explore the application of this noise-leveraging technique within hybrid quantum neural networks, particularly for advancing performance in industrial tasks such as image processing [42–44], time series forecasting [45, 46], and planning [47, 48].

-
- [1] Sergey Bravyi, Oliver Dial, Jay M. Gambetta, Darío Gil, and Zaira Nazario. The future of quantum computing with superconducting qubits. *Journal of Applied Physics*, 132(16), 2022.
 - [2] Colin D. Bruzewicz, John Chiaverini, Robert McConnell, and Jeremy M. Sage. Trapped-ion quantum computing: Progress and challenges. *Applied Physics Reviews*, 6(2), 2019.
 - [3] Anasua Chatterjee, Paul Stevenson, Silvano De Franceschi, Andrea Morello, Nathalie P. de Leon, et al. Semiconductor qubits in practice. *Nature Reviews Physics*, 3(3):157–177, 2021.
 - [4] John Preskill. Quantum computing in the NISQ era and beyond. *Quantum*, 2:79, 2018.
 - [5] Mohammad Kordzanganeh, Markus Buchberger, Basil Kyriacou, Maxim Povolotskii, Wilhelm Fischer, et al. Benchmarking simulated and physical quantum processing units using quantum and hybrid algorithms. *Advanced Quantum Technologies*, 6(8):2300043, 2023.
 - [6] Mikio Namiki, Saverio Pascazio, and Hiromichi Nakazato. *Decoherence and quantum measurements*. World Scientific, 1997.
 - [7] Leonid Fedichkin, Arkady Fedorov, and Vladimir Privman. Measures of decoherence. In *Quantum Information and Computation*, volume 5105, pages 243–254. SPIE, 2003.
 - [8] Arkady Fedorov, Leonid Fedichkin, and Vladimir Privman. Evaluation of decoherence for quantum control and computing. *Journal of Computational and Theoretical Nanoscience*, 1(2):132–143, 2004.
 - [9] Jinfeng Zeng, Zipeng Wu, Chenfeng Cao, Chao Zhang, Shi-Yao Hou, et al. Simulating noisy variational quantum eigensolver with local noise models. *Quantum Engineering*, 3(4):e77, 2021.
 - [10] Andrea Skolik, Stefano Mangini, Thomas Bäck, Chiara Macchiavello, and Vedran Dunjko. Robustness of quantum reinforcement learning under hardware errors. *EPJ Quantum Technology*, 10(1):1–43, 2023.
 - [11] Daniel Azses, Maxime Dupont, Bram Evert, Matthew J. Reagor, and Emanuele G. Dalla Torre. Navigating the noise-depth tradeoff in adiabatic quantum circuits. *Physical Review B*, 107(12):125127, 2023.
 - [12] Chen Ding, Xiao-Yue Xu, Shuo Zhang, He-Liang Huang, and Wan-Su Bao. Evaluating the resilience of variational quantum algorithms to leakage noise. *Physical Review A*, 106(4):042421, 2022.
 - [13] Junyu Liu, Frederik Wilde, Antonio Anna Mele, Liang Jiang, and Jens Eisert. Stochastic noise can be helpful for variational quantum algorithms. *arXiv preprint arXiv:2210.06723*, 2022.
 - [14] Yuxuan Du, Min-Hsiu Hsieh, Tongliang Liu, Dacheng Tao, and Nana Liu. Quantum noise protects quantum classifiers against adversaries. *Physical Review Research*, 3:023153, 2021.
 - [15] L. Domingo, G. Carlo, and F. Borondo. Optimal quantum reservoir computing for the noisy intermediate-scale quantum era. *Physical Review E*, 106:L043301, 2022.
 - [16] Chris M. Bishop. Training with Noise is Equivalent to Tikhonov Regularization. *Neural Computation*, 7(1):108–116, 1995.
 - [17] Guozhong An. The Effects of Adding Noise During Backpropagation Training on a Generalization Performance. *Neural Computation*, 8(3):643–674, 1996.
 - [18] Arvind Neelakantan, Luke Vilnis, Quoc V Le, Ilya Sutskever, Lukasz Kaiser, et al. Adding gradient noise improves learning for very deep networks. *arXiv preprint arXiv:1511.06807*, 2015.
 - [19] Maria Schuld and Francesco Petruccione. *Machine learning with quantum computers*, volume 676. Springer, 2021.
 - [20] Alexey Melnikov, Mohammad Kordzanganeh, Alexander Alodjants, and Ray-Kuang Lee. Quantum machine learning: from physics to software engineering. *Advances in Physics: X*, 8(1):2165452, 2023.
 - [21] Valentin Heyraud, Zejian Li, Zakari Denis, Alexandre Le Boité, and Cristiano Ciuti. Noisy quantum kernel machines. *Physical Review A*, 106:052421, 2022.
 - [22] Nam H. Nguyen, Elizabeth C. Behrman, and James E. Steck. Quantum learning with noise and decoherence: a robust quantum neural network. *Quantum Machine Intelligence*, 2(1):1, 2020.
 - [23] F. Pedregosa, G. Varoquaux, A. Gramfort, V. Michel, B. Thirion, et al. Scikit-learn: Machine learning in Python. *Journal*

- of *Machine Learning Research*, 12:2825–2830, 2011.
- [24] Bradley Efron, Trevor Hastie, Iain Johnstone, and Robert Tibshirani. Least angle regression. *The Annals of Statistics*, 32(2):407–499, 2004.
- [25] Kerstin Beer, Dmytro Bondarenko, Terry Farrelly, Tobias J. Osborne, Robert Salzmann, et al. Training deep quantum neural networks. *Nature Communications*, 11(1):808, 2020.
- [26] Matthias C. Caro, Hsin-Yuan Huang, M. Cerezo, Kunal Sharma, Andrew Sornborger, et al. Generalization in quantum machine learning from few training data. *Nature Communications*, 13(1):4919, 2022.
- [27] Iris Cong, Soonwon Choi, and Mikhail D. Lukin. Quantum convolutional neural networks. *Nature Physics*, 15(12):1273–1278, 2019.
- [28] Mo Kordzanganeh, Pavel Sekatski, Leonid Fedichkin, and Alexey Melnikov. An exponentially-growing family of universal quantum circuits. *Machine Learning: Science and Technology*, 4(3):035036, 2023.
- [29] Mo Kordzanganeh, Daria Kosichkina, and Alexey Melnikov. Parallel hybrid networks: an interplay between quantum and classical neural networks. *Intelligent Computing*, 2:0028, 2023.
- [30] Asel Sagingalieva, Mohammad Kordzanganeh, Nurbolat Kenbayev, Daria Kosichkina, Tatiana Tomashuk, et al. Hybrid quantum neural network for drug response prediction. *Cancers*, 15(10):2705, 2023.
- [31] Alexandr Sedykh, Maninadh Podapaka, Asel Sagingalieva, Karan Pinto, Markus Pflitsch, et al. Hybrid quantum physics-informed neural networks for simulating computational fluid dynamics in complex shapes. *Machine Learning: Science and Technology*, 5(2):025045, 2024.
- [32] Matvei Anoshin, Asel Sagingalieva, Christopher Mansell, Dmitry Zhiganov, Vishal Shete, et al. Hybrid quantum cycle generative adversarial network for small molecule generation. *IEEE Transactions on Quantum Engineering*, 5:2500514, 2024.
- [33] Ville Bergholm, Josh Izaac, Maria Schuld, Christian Gogolin, Shah Nawaz Ahmed, et al. PennyLane: Automatic differentiation of hybrid quantum-classical computations. *arXiv preprint arXiv:1811.04968*, 2018.
- [34] Diederik Kingma and Jimmy Ba. Adam: A method for stochastic optimization. In *International Conference on Learning Representations (ICLR)*, San Diego, CA, USA, 2015.
- [35] Adam Paszke, Sam Gross, Francisco Massa, Adam Lerer, James Bradbury, et al. PyTorch: An imperative style, high-performance deep learning library. In *Advances in Neural Information Processing Systems 32*, pages 8024–8035. Curran Associates, Inc., 2019.
- [36] Preetum Nakkiran, Gal Kaplun, Yamini Bansal, Tristan Yang, Boaz Barak, et al. Deep double descent: Where bigger models and more data hurt. *Journal of Statistical Mechanics: Theory and Experiment*, 2021(12):124003, 2021.
- [37] Rigetti Staff. Rigetti QCS, 2022.
- [38] IonQ. Amazon Braket - Aria 1, 2023.
- [39] IonQ Staff. IonQ Aria: Practical Performance, 2023.
- [40] Frank Arute, Kunal Arya, Ryan Babbush, Dave Bacon, Joseph C. Bardin, et al. Quantum supremacy using a programmable superconducting processor. *Nature*, 574(7779):505–510, 2019.
- [41] IBM Staff. IBM Quantum, 2023.
- [42] Asel Sagingalieva, Andrii Kurkin, Artem Melnikov, Daniil Kuhmistrov, et al. Hybrid quantum ResNet for car classification and its hyperparameter optimization. *Quantum Machine Intelligence*, 5(2):38, 2023.
- [43] Luca Lusnig, Asel Sagingalieva, Mikhail Surmach, Tatjana Protasevich, Ovidiu Michiu, et al. Hybrid quantum image classification and federated learning for hepatic steatosis diagnosis. *Diagnostics*, 14(5):558, 2024.
- [44] Arsenii Senokosov, Alexandr Sedykh, Asel Sagingalieva, Basil Kyriacou, and Alexey Melnikov. Quantum machine learning for image classification. *Machine Learning: Science and Technology*, 5(1):015040, 2024.
- [45] Asel Sagingalieva, Stefan Komorniyk, Arsenii Senokosov, Ayush Joshi, Alexander Sedykh, et al. Photovoltaic power forecasting using quantum machine learning. *arXiv preprint arXiv:2312.16379*, 2023.
- [46] Andrii Kurkin, Jonas Hegemann, Mo Kordzanganeh, and Alexey Melnikov. Forecasting the steam mass flow in a powerplant using the parallel hybrid network. *arXiv preprint arXiv:2307.09483*, 2023.
- [47] Serge Rainjonneau, Igor Tokarev, Sergei Iudin, Saaketh Rayaprolu, Karan Pinto, et al. Quantum algorithms applied to satellite mission planning for Earth observation. *IEEE Journal of Selected Topics in Applied Earth Observations and Remote Sensing*, 16:7062–7075, 2023.
- [48] Nathan Haboury, Mo Kordzanganeh, Sebastian Schmitt, Ayush Joshi, Igor Tokarev, et al. A supervised hybrid quantum machine learning solution to the emergency escape routing problem. *arXiv preprint arXiv:2307.15682*, 2023.